Fibrin-filled scaffolds for bone-tissue engineering: An *in vivo* study

Jeffrey M. Karp,[1,2] Feryal Sarraf,[1,3] Molly S. Shoichet,[1,2] John E. Davies [1,2,3]
[1]*Institute of Biomaterials and Biomedical Engineering, University of Toronto, 4 Taddle Creek Road, Toronto, Ontario, Canada M5S 3G9*
[2]*Department of Chemical Engineering and Applied Chemistry, University of Toronto, 200 College Street, Toronto, Ontario, Canada M5S 3E5*
[3]*Faculty of Dentistry, University of Toronto, 124 Edward Street, Toronto, Ontario, Canada M5G 1G6*

Received 25 March 2004; revised 7 June 2004; accepted 16 June 2004
Published online 9 August 2004 in Wiley InterScience (www.interscience.wiley.com). DOI: 10.1002/jbm.a.30147

Abstract: Recently, fibrin sealants that typically contain supra physiological concentrations of fibrinogen and thrombin have been investigated as matrices to facilitate the delivery of cells within biodegradable scaffolds for tissue engineering applications. It is well known from *in vitro* experiments that the thrombin concentration present during fibrin polymerization influences the structural properties of fibrin, and these can affect cell invasion. This study was conducted to determine whether the structural properties of fibrin can affect bony wound healing *in vivo*. Drill hole defects were created in the distal femurs of 20 rats. Four experimental groups were used: nontreated defects, scaffolds alone, and scaffolds filled with fibrin polymerized with either a low thrombin concentration [fibrin(low T)] or a high thrombin concentration [fibrin(high T)]. The area of bone formed at 2, 5, and 11 days after implantation was determined histomorphometrically. After 5 days, scaffolds filled with fibrin(high T) were infiltrated with less bone than empty scaffolds ($p < 0.05$), but no statistical difference was found between the empty scaffolds and the scaffolds filled with fibrin(low T). After 11 days, both fibrin-filled scaffolds significantly delayed bony wound healing ($p < 0.004$). Reducing sodium dodecyl sulfate polyacrylamide gel electrophoresis analysis of the two fibrin formulations showed no difference in γ-γ crosslink formation. This work demonstrates that fibrin sealants in their present state are not ideal for enhancing bone-tissue invasion into scaffolds, and that the structural properties of fibrin matrices may be an important design parameter for maximizing host tissue invasion during wound healing. © 2004 Wiley Periodicals, Inc. J Biomed Mater Res 71A: 162–171, 2004

Key words: biodegradable polymer; composite; matrix structure; thrombin concentration; wound healing

INTRODUCTION

Within the past three decades, there has been great interest in using fibrin sealants (FSs) to clinically augment skeletal wound healing by combining them with autologous and allogenic bone grafts,[1,2] antibiotics,[3] and hydroxyapatite particles.[4] FSs are prepared from plasma pooled from a large number of human donors and typically contain 10–20 times the physiological concentration of fibrinogen and high concentrations of thrombin, in addition to additives such as factor XIII to crosslink the fibrin and aprotinin to decrease the rate of degradation. They have been demonstrated in animal models to accelerate neovascularization[5] and to help improve the surgical handling properties of graft materials such as demineralized bone powder,[6] bioactive glass,[7] hydroxyapatite,[8] and coral granules.[9] In addition, FSs have been demonstrated to be effective delivery vehicles for bioactive agents such as transforming growth factor-β-1[10] and transforming growth factor-β-related bone morphogenetic proteins.[11]

Recently, FSs have been investigated as matrices to facilitate the delivery of cells for tissue engineering applications.[10,12–18] For some of these cell delivery strategies, the fibrin and cells are combined with biodegradable scaffolds,[10,12,16,18] which is especially useful in scaffolds that do not permit cell adhesion.[17] Although FSs may be useful as delivery vehicles for cells, and given that fibrin releases chemotactic agents when it forms and degrades,[19–21] the affects of FS on bony wound healing have not been consistent[5,22–26]

Correspondence to: J. E. Davies; e-mail: davies@ecf.utoronto.ca

Contract grant sponsor: Ontario Research and Development Challenge Fund (to JED)
Contract grant sponsor: Ontario Graduate Scholarship (to JMK)

and their role in wound healing is not fully understood.[26]

In addition to the variability in fibrin compositions used *in vivo*,[23,24,27,28] the properties of the fibrin that are relevant to host tissue invasion have generally been ignored. Most FSs are supplied with only one formulation,[29] which is primarily designed to stop bleeding and provide adhesive properties. Yet, FSs are being investigated to enhance wound healing of various tissues without modifying the matrix to suit the intended application.[10,12–17] The majority of FSs contain a high thrombin concentration,[29] which results in a network of thin short fibers and small pores.[30] Thin fibers and small pores have been shown to significantly reduce cell migration *in vitro* compared with fibrin gels with thick fibers and larger pores[31,32]; thus, it is important to consider that not all polymerized fibrin formulations are equally cell invasive.[33] To gain insight into the role of fibrin architecture *in vivo*, we compared the bony wound healing achieved using FS formed with thin fibers and small pores to FS formed with thick fibers and large pores. To help immobilize the FS within the *in vivo* defect site, we combined it with highly interconnecting, macroporous, biodegradable poly(lactide-*co*-glycolide) (PLGA) scaffolds. We hypothesized that PLGA scaffolds filled with FS having thick fibrin strands and large pores, that is, formed with a low thrombin concentration, would facilitate more rapid bony wound healing than scaffolds filled with FS having thin fibrin strands and small pores, that is, formed with a high thrombin concentration.

To test our hypothesis, we implanted fibrin-filled scaffolds into small drill hole defects in the distal femur of rats. This model, which we have previously demonstrated to be useful for testing scaffolds for bone-tissue-engineering applications,[34] was chosen because of its relative simplicity. The results from the fibrin-filled scaffold groups were compared with defects containing empty scaffolds and unfilled defect controls. Furthermore, the degree of fibrin crosslinking was characterized by reducing sodium dodecyl sulfate polyacrylamide gel electrophoresis (SDS-PAGE) analysis because thrombin activates coagulation factor XIII which catalyzes covalent crosslink formation in fibrin clots, and this can affect cell invasion.[35,36]

MATERIALS AND METHODS

Scaffold fabrication

Composite PLGA 75:25 scaffolds containing calcium phosphate (CaP) were produced by modifying a previously described technology.[34] Briefly, an equimolar mixture of dicalcium and tetracalcium phosphate was reacted to form hydroxyapatite, and this was crushed into small particles and sieved. Particles less than 45 μm were dispersed with glucose crystals having 0.85- to 1.18-mm dimensions in a solution of 11.5% (w/v) PLGA (inherent viscosity of 1.13 dL/g), in dimethylsulfoxide. The ratio of CaP/PLGA was 2:1 (wt/wt). The sugar/polymer/CaP mixture was placed in a Teflon® fluorinated ethylene propylene-coated aluminum foil mold, allowed to set at −20°C, and then placed into water at room temperature. Scaffolds were cut into cylindrical shapes using methods previously published.[34]

Filling scaffolds with FS

The FS Tisseel® VH (Baxter Biosciences, Canada) is supplied in Canada with two different thrombin concentrations (220 or 1.75 NIH U/mL) and each of these was used resulting in fibrin(high T)- and fibrin(low T)-filled scaffolds, respectively. After reconstitution and mixing of all the supplied reagents (at 37°C), FS consisted of: 35–55 mg/mL fibrinogen, 1.75 or 220 NIH U/mL thrombin, 5–25 U/mL factor XIII, and 1500 KIU/mL bovine aprotinin.

After the precut scaffolds were wetted in 70% EtOH and rinsed in ddH_2O three times, 15 μL of fibrinogen-containing solution was added to the scaffolds followed by 15 μL of the thrombin-containing solution. These solutions were quickly mixed in the scaffold and the resulting fibrin was allowed to gel in an incubator for 1 h. Fibrin-filled scaffolds were selected for *in vivo* implantation based on the presence of fibrin at the margins of all scaffold surfaces, as observed using a dissecting microscope. Filling the scaffolds with fibrin caused approximately a 20% increase in scaffold diameter. The selected fibrin-filled scaffolds in addition to the empty scaffolds were placed into an aprotinin (1500 KIU/mL, Sigma Chemical Company) α-minimal essential medium solution and incubated for 12 h. All scaffolds were filled with Tisseel® FS from the same lot number.

Scanning electron microscopy (SEM)

SEM was used to confirm that the thrombin concentration affected fibrin structural properties as previously demonstrated[31] and that the PLGA-CaP scaffolds were filled with fibrin. Fibrin-filled scaffolds were rinsed twice with 0.1*M* sodium cacodylate buffer (pH 7.4, 37°C) and fixed for 30 min in Karnovsky's fixative at 4°C. After rinsing with cacodylate buffer three times, the fibrin-filled scaffolds were dehydrated in graded alcohol solutions, freeze fractured, and then critical point dried from CO_2. The samples were then sputter-coated with platinum (≈10 nm) and examined by a scanning electron microscope at 10 kV (Hitachi 2500).

Electrophoresis

FSs were processed for reducing conditions by SDS-PAGE on 4–12% NuPAGE BisTris gels (Invitrogen, Burlington,

TABLE I
Treatment and Randomization Table

	2 Days	5 Days	11 Days
Empty defect	3 (5L, 6L, 7R)	3 (15L, 16L, 17R)	3 (19L, 18R, 20R)
Empty scaffold	3 (7L, 2R, 3R)	3 (17L, 12R, 13R)	3 (20L, 9R, 10R)
Fibrin-filled scaffold (low T)	4 (2L, 4L, 1R, 5R)	4 (12L, 14L, 11R, 15R)	3 (9L, 18L, 8R)
Fibrin-filled scaffold (high T)	4 (1L, 3L, 4R, 6R)	4 (11L, 13L, 14R, 16R)	3 (8L, 10L, 19R)

Data are number of defects per experimental group and (rat no. left [L] and right [R] femur).

Ontario). In brief, 20-μL fibrin gels were produced by combining 10 μL of fibrinogen with 10 μL of thrombin at 37°C. The reaction was stopped either immediately, after 30 min, or after 12 h by the addition of 4 m*M* ethylenediaminetetraacetic acid (three times). The matrices were incubated with 500 μL of solubilizing buffer (8*M* urea, 2% SDS, 40 m*M* dithiothreitol, 2 m*M* ethylenediaminetetraacetic acid) at 100°C for 10 min and then 25 μL of each extract was used for separation on reducing SDS-PAGE. The fibrinogen-containing solution (10 μL) served as a negative control for γ-γ crosslinking. This experiment was performed two times with individual packages of FS from the same lot number.

In vivo model

Bone defects were made in the distal femora to accommodate fibrin-filled scaffolds using a dental drill (2.3 mm in diameter) with copious saline irrigation. The cylindrical scaffolds (2.6 mm in diameter × 3.45 mm in height) were implanted into the bone defects in the mid-diaphysis of both the right and left femora of 20 adult (4-month-old) male Brown Norway rats. The interstices of empty scaffolds were, upon implantation, filled with blood, which clotted and maintained them *in situ*. The rats were inbred for at least 10 generations and can be considered homozygous for virtually all loci. The maintenance and use of animals were in accordance with the Canadian Council of Animal Care Guidelines. A sample size of three or four was used for each group, and rats were randomized to treatment groups according to Table I. The femora were subsequently fixed in formalin for 48 h, decalcified, dehydrated, and embedded in low-melting-point paraffin. The paraffin blocks were sectioned perpendicular to the long axis of each scaffold using a hard tissue Spencer 820 microtome. After sectioning through almost the first half of each block, 12–16 sections were obtained from three areas that were each at least 120 μm apart. This ensured that sections were obtained from the middle of all defects. Sections were stained with either toluidine blue to identify general structures or a Masson's trichrome to identify the collagen component of bone. Some sections were stained with a picrosirius red (PSR) stain and observed with polarizing filters to detect birefringence from the collagen.

Histomorphometry

Representative sections, as illustrated in the figures with their absolute field widths, were selected from each of the three areas in the middle of the defect and enlarged to ×70 magnification on a computer screen to undertake histomorphometry using Image Pro Plus 4.1 (Media Cybernetics, Silver Spring, MD). This computer program was used to identify bone tissue by its blue staining (Masson's trichrome). The selected area was then visually confirmed as bone by its morphological similarity to trabecular bone adjacent to the defect site and by visually confirming the presence of osteocytes. Residual FS appeared light gray because of a lack of appreciable staining. Areas occupied by the scaffold were identified by their bright white appearance and by the presence of irregularly distributed cells within the scaffold micropores. Clusters of blood cells were identified by their bright red or red-brown appearance at low magnification whereas individual red blood cells were identified at a higher magnification. Sections acquired from three separate areas within the center of the defect were used to calculate an average parametric value for each femur. Averages were obtained from three sections, from each of the three areas in the middle of each defect to obtain individual values, and this was repeated for three or four samples (n = 3 or 4 as in Table I). Histomorphometric calculations were performed according to Equations (1) to (4):

$$\%\ \text{Available Area Occupied by Bone} = \frac{\text{Area}_{\text{Bone}}}{\text{Area}_{\text{Defect}} - \text{Area}_{\text{Scaffold}}} \quad (1)$$

$$\%\ \text{Available Area Occupied by High Concentrations of Blood Cells} = \frac{\text{Area}_{\text{BloodCells}}}{\text{Area}_{\text{Defect}} - \text{Area}_{\text{Scaffold}}} \quad (2)$$

$$\%\ \text{Available Area Occupied by Fibrin Sealant} = \frac{\text{Area}_{\text{Fibrin}}}{\text{Area}_{\text{Defect}} - \text{Area}_{\text{Scaffold}}} \quad (3)$$

$$\%\ \text{Area Occupied by The Scaffold} = \frac{\text{Area}_{\text{Scaffold}}}{\text{Area}_{\text{Defect}}} \quad (4)$$

Statistical analysis

All measurements were collected from triplicate sections from either three or four defects per experimental group and expressed as means ± standard deviation. For multiple comparisons, analysis of variance was performed with the

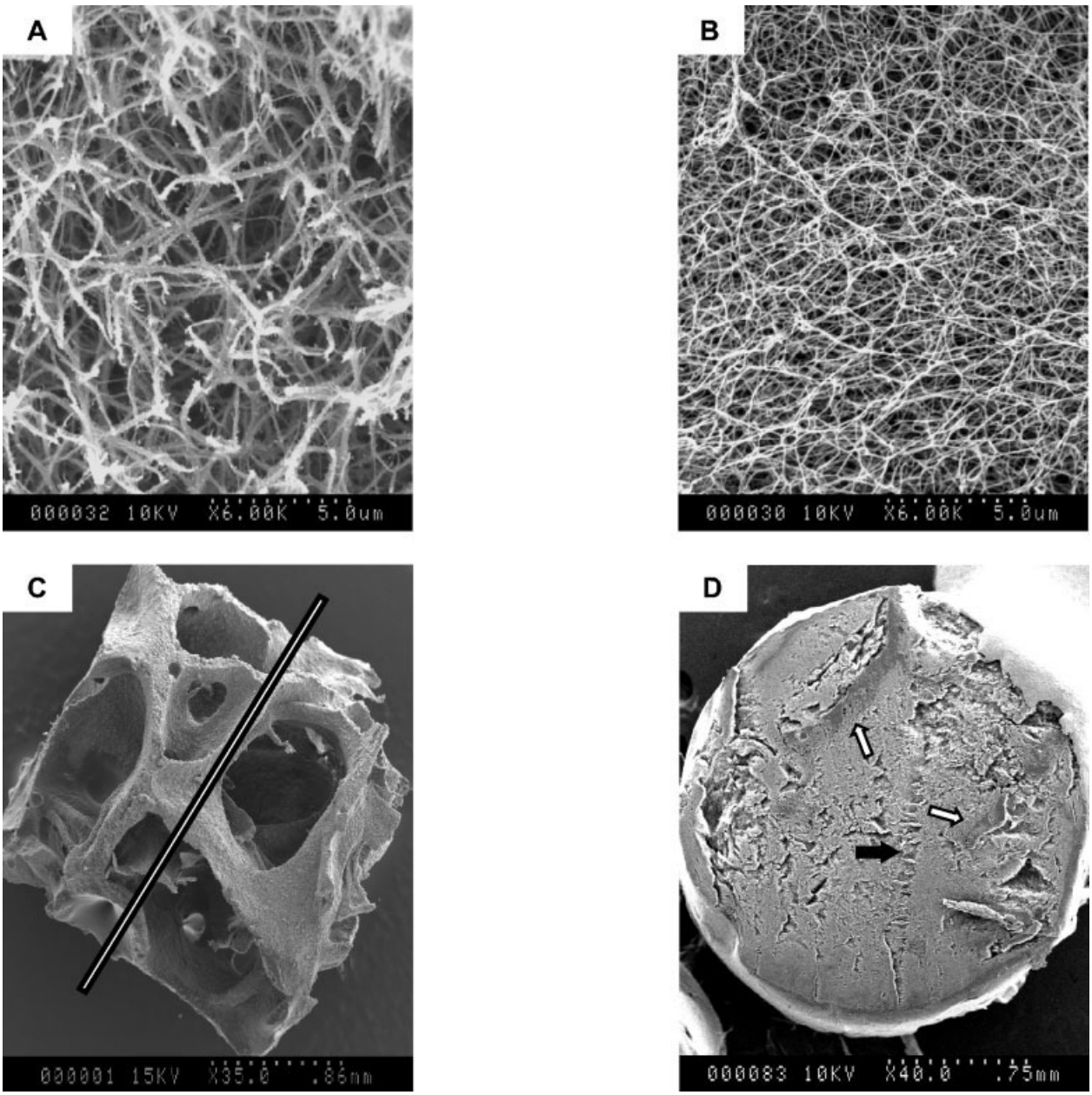

Figure 1. Scanning electron micrographs of (A) fibrin polymerized with a low thrombin concentration (1.75 NIH U/mL) contained thicker fibrin strands with larger pores than (B) fibrin polymerized with a high thrombin concentration (220 NIH U/mL). (C) An empty scaffold viewed longitudinally and (D) a fibrin-filled scaffold cross-section. The latter (D) was taken in the center of the fibrin-filled scaffold [see white line in (C)] and demonstrates that scaffolds were completely filled with fibrin. The white arrows point to the scaffold, whereas the black arrow points to a knife mark created from cutting through the center of fibrin-filled scaffolds.

Tukey test, and the Student *t* test was used to make pairwise comparisons at significance levels of 95%.

RESULTS

SEM

Freeze-fractured fibrin-filled scaffolds were examined by SEM (Fig. 1). Fibrin(low T) was observed to have larger pores (≈2 μm) and thicker fibrin strands (each visible strand comprised multiple fibrin fibers) [Fig. 1(A)] than fibrin(high T) which had smaller pores (≈0.5 μm) and thinner fibrin strands [Fig. 1(B)]. SEM was also used to confirm that PLGA scaffolds [Fig. 1(C)] were completely filled with FS [Fig. 1(D)], before the *in vivo* work. The scaffolds had a high degree of interconnecting macroporosity with pore sizes ranging from 0.85 to 1.18 mm in diameter. When filled with fibrin, it became difficult to distinguish between the scaffold and the fibrin [Fig. 1(D)] which is likely due to sample preparation.

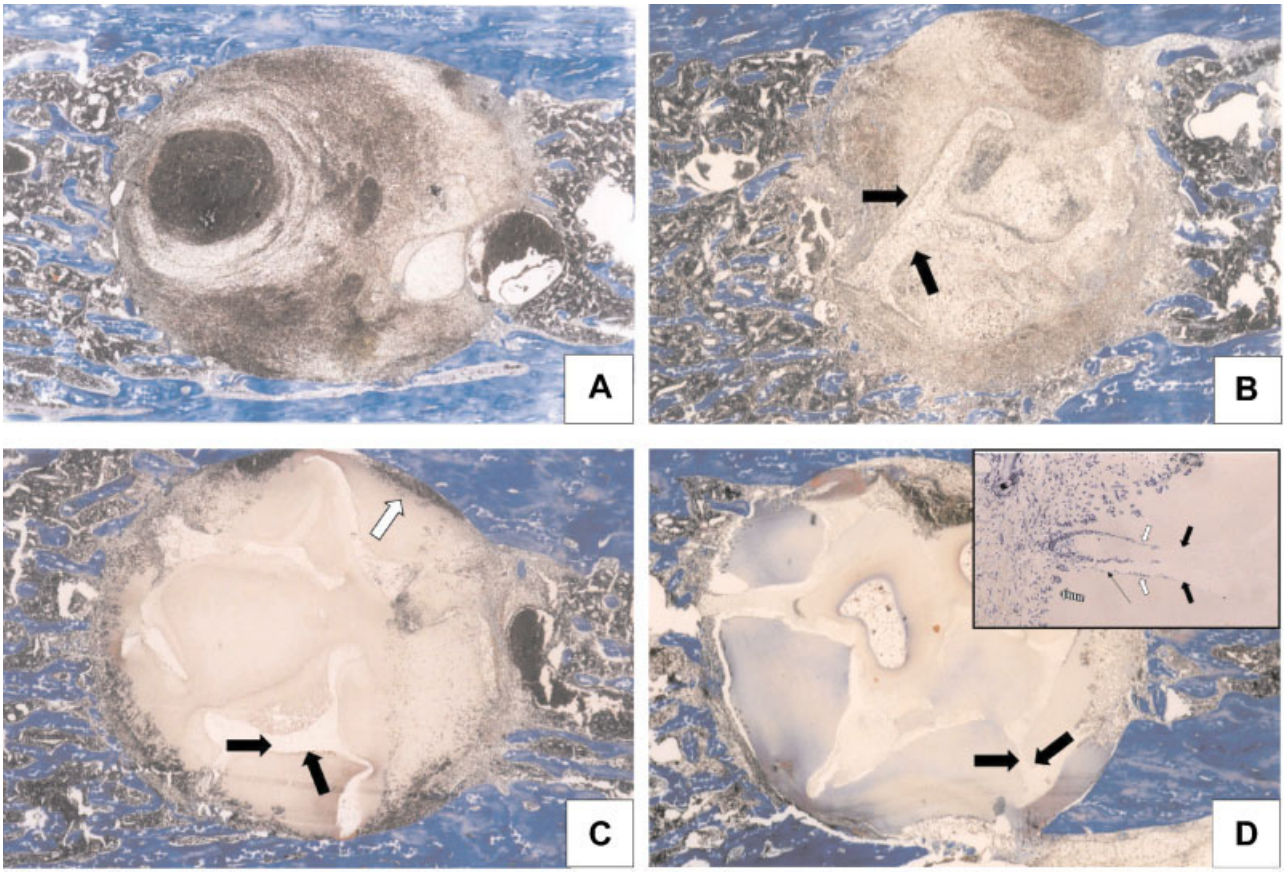

Figure 2. Masson's trichrome-stained sections after 2 days *in vivo*. (A) Untreated defects contained a high concentration of blood cells whereas a much lower concentration was observed in the pores of the empty scaffolds. (B) Filling scaffolds with both fibrin(low T) (C) and fibrin(high T) (D) significantly decreased the number of blood cells trapped within the defect. No reparative bone was observed at this time in any of the defects. The black arrows point to areas occupied by the scaffold and the white arrows point to mononuclear cells at the fibrin/defect interface. Inset: toluidine blue-stained sections revealed that mononuclear cells preferred migrating along the polymer surface of scaffolds filled with fibrin(high T) than through the fibrin. In some areas, the fibrin detached from the scaffold, which is likely an artifact created during histological processing (skinny black arrow). White arrows and striped arrows indicate cells migrating along the fibrin/scaffold interface and through the fibrin, respectively. Black arrows point to the position of the scaffold. Field width = 5.2 mm, inset field width = 1.2 mm. [Color figure can be viewed in the online issue, which is available at www.interscience.wiley.com.]

Histology

After 2 days *in vivo*, the untreated defects [Fig. 2(A)] were filled with clotted blood. Empty scaffolds contained a lower concentration of blood clot within the scaffold pores compared with the bulk area of the untreated defects [Fig. 2(B)]. An inflammatory response was observed in regions at the scaffold interface as evidenced by the presence of a dense population of neutrophils that were identified by their highly lobed mononuclei. Histology confirmed that the FS completely filled the scaffold pores for both fibrin-filled scaffold groups and this limited the space occupied by the blood clot to margins in the defect site [Fig. 2(C,D)]. An inflammatory response was also observed in both fibrin-filled scaffold groups, although this response was restricted to the edges of the defect. As expected, the presence of FS within the scaffold pores significantly limited the immediate interaction of cells with the scaffold. In defects containing scaffolds filled with fibrin(low T), mononuclear cells were observed migrating from the periphery of the defect through the fibrin [Fig. 2(C)]. In contrast to the scaffolds filled with fibrin(low T), mononuclear cells did not penetrate as far into defects containing scaffolds filled with fibrin-(high T) [Fig. 2(D)]; cells migrated further along the scaffold fibrin interface than into the fibrin [Fig. 2(D), inset].

After 5 days *in vivo*, blood clot remained in the center of untreated defects (not shown). An acute inflammatory response was evident in multiple areas juxtaposed to the scaffold surface, for all scaffold-containing groups, and was also evident juxtaposed to areas containing residual FS. Multinucleated giant cells were observed in regions at the scaffold interface for all scaffold-containing groups. Bone was observed infiltrating from the periphery of the defects in all groups, although there was considerably less identifi-

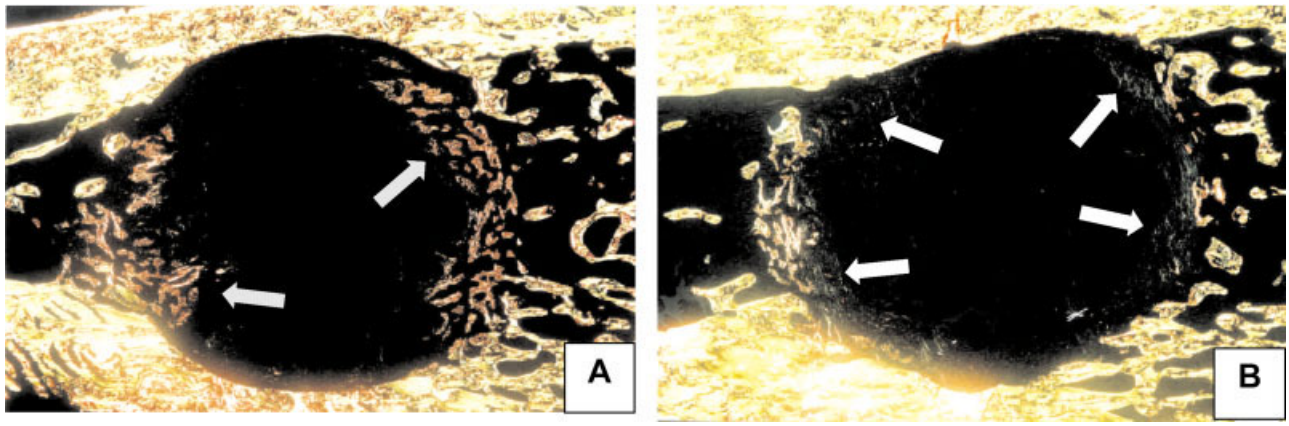

Figure 3. Five-day PSR-stained sections observed under polarized light. (A) Reparative bone at the periphery of scaffolds filled with fibrin(low T) was bright red-orange (gray arrows), which indicates the presence of thick, mature collagen fibers. (B) Collagen fibers at the periphery of scaffolds filled with fibrin(high T) were green (white arrows), which indicates that they were thin and less mature. Field width = 5.2 mm. [Color figure can be viewed in the online issue, which is available at www.interscience.wiley.com.]

able reparative bone in the scaffolds filled with fibrin-(high T). This fibrin-filled scaffold group contained a greater amount of residual FS. In both fibrin-filled scaffold groups, cells were clearly identified invading deep into the defects, occupying areas once filled with fibrin (not shown).

To more clearly identify the collagen component of bone, sections were stained with PSR which enhances the natural birefringent properties of collagen under polarized light and allows identification of very thin fibrils that are not detectable in normal microscopy.[37] Comparison of the two fibrin-filled scaffold groups after 5 days *in vivo* with polarized light (Fig. 3) indicated that scaffolds filled with fibrin(high T) contained fine collagen fibers near the periphery of the defect that were a distinct green color.[38] These fibers were disordered in contrast to the invading trabecular bone which was observed in the scaffolds filled with fibrin-(low T). Cortical bone and new and old trabecular bone displayed a high level of birefringence and were either bright yellow, orange, or red, which is characteristic of organized bundles of collagen fibers.

After 11 days *in vivo* (Fig. 4), bone was clearly observed throughout the untreated defects [Fig. 4(A)] and throughout the pores of the empty scaffolds [Fig. 4(B)]. Although the acute inflammatory response observed at days 2 and 5 had subsided, multinucleated giant cells were still present at the scaffold surface for all scaffold-containing groups [Fig. 4(B), inset]. Negligible amounts of FS were detected within scaffolds filled with fibrin(low T) whereas small areas remained defects containing scaffolds with fibrin(high T) (not shown). Although similar amounts of bone were observed within the fibrin-filled scaffold groups [Fig. 4(C,D)], no bone was observed at the center of these defects.

Electrophoresis

Reducing SDS-PAGE analysis of the Tisseel® FS (Fig. 5) revealed that the fibrinogen control (lane 1) contained peaks for Aα, Bβ, and γ-monomers, yet no γ-dimers. When the fibrin polymerization reaction was stopped after 2 min, fibrin(low T) (lane 2) contained fewer γ-dimers and more γ-monomers than fibrin(high T) (lane 3). After 30 min of polymerization, the γ-dimer peak for fibrin(low T) (lane 4) increased whereas the γ-monomers decreased; for fibrin(high T) (lane 5), all of the γ chains were converted to γ-dimers. Although the γ-dimer peak for fibrin(low T) (lane 4) had increased, γ-monomers remained. After a 12-h incubation, most of the γ-monomers were crosslinked into γ-dimers for both fibrin(low T) (lane 6) and fibrin-(high T) (lane 7) and most of the Aα chains had been ligated.

Histomorphometric analysis

After 5 days *in vivo*, less bone had infiltrated the scaffolds containing fibrin(high T) than the empty scaffold group ($p < 0.05$) and the scaffolds filled with fibrin(low T) ($p < 0.08$) (Fig. 6). This correlated with the remodeling of the FS observed between the 2- and 5-day time points ($p < 0.06$). Specifically, 62% of the defect area, which was filled with fibrin(low T) on day 2 had been replaced with new connective tissue and cells by day 5 compared with only 34% for the scaffolds filled with fibrin(high T). There was no statistical difference in the quantity of reparative bone found at 5 days between untreated defects, empty scaffolds, and defects containing scaffolds filled with fibrin(low

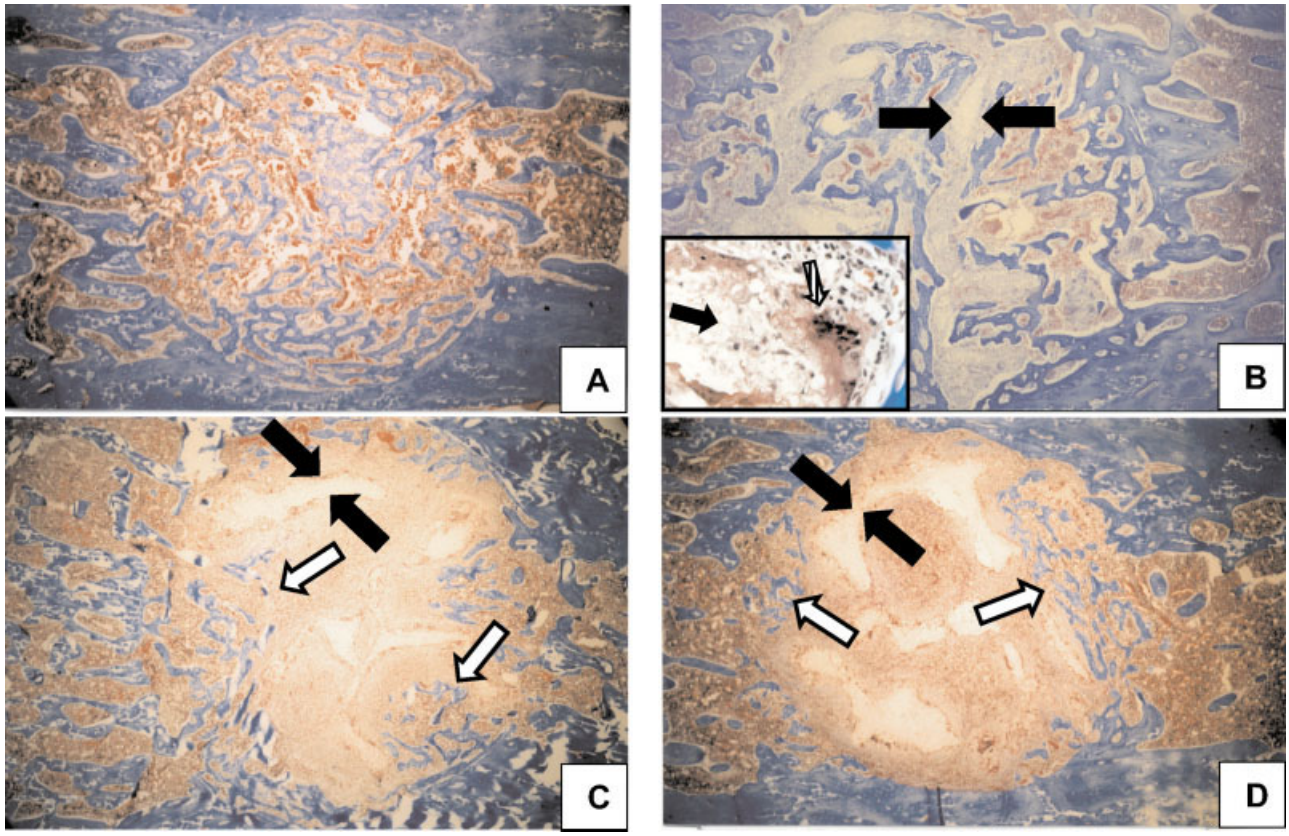

Figure 4. Eleven-day Masson's trichrome-stained sections. (A) Untreated defects and (B) defects containing empty scaffolds were filled with new bone tissue. However, no reparative bone was observed in the center of defects containing (C) scaffolds filled with fibrin(low T) and (D) scaffolds filled with fibrin(high T). (Inset) Patches of multinucleated giant cells (striped arrow) were observed at the scaffold interface in all scaffold-containing groups. Black arrows point to areas occupied by the scaffold, whereas white arrows point to the advancing bone front. Field width = 5.2 mm, inset field width = 0.2 mm. [Color figure can be viewed in the online issue, which is available at www.interscience.wiley.com.]

T). Although all groups had a significant increase in bone infiltration between days 5 and 11 (Fig. 6), the empty defect and empty scaffold groups contained more reparative bone at day 11 compared with both fibrin-filled scaffold groups ($p < 0.004$).

The area of blood clot that filled the defect was quantified by measuring the percent area occupied by clusters of blood cells. The untreated defects filled with more blood (33 ± 7%) than the empty scaffolds (11 ± 1%), the scaffolds filled with fibrin(low T) (3 ± 1%), and the scaffolds filled with fibrin(high T) (5 ± 2%) as evidenced after 2 days *in vivo* ($p < 0.001$). After 5 days, all groups had significantly less clusters of blood cells, although the untreated defects contained significantly more clusters than the other groups ($p < 0.04$). Over the 11-day time period *in vivo*, the scaffold did not appear to degrade.

DISCUSSION

We determined that the structural properties of FSs influence the early *in vivo* wound-healing response. Specifically, bone-tissue invasion was more rapid during the first 5 days of healing within scaffolds filled with fibrin(low T) (8.1% of available area occupied by bone) (Figs. 3 and 6) compared with scaffolds filled with fibrin(high T) (2.2% of available area occupied by bone); this correlated with an increased rate of FS remodeling for the scaffolds filled with fibrin(low T) (62% reduction in defect area occupied by fibrin) compared with the scaffolds filled with fibrin(high T) (34% reduction in defect area occupied by fibrin). We detected more disorganized thin collagen fibrils within scaffolds filled with fibrin(high T) compared with scaffolds filled with fibrin(low T) at 5 days by taking advantage of collagen's birefringent properties using PSR-stained sections viewed under polarized light (Fig. 3). This immature matrix was remodeled into bone by 11 days *in vivo* [Fig. 4(D)]. Although it is difficult to determine whether the loosely organized collagen matrix observed after 5 days was immature bone or fibrous tissue, it is evident that scaffolds filled with fibrin(high T) experienced delayed bony wound healing.

The differences observed between the two fibrin

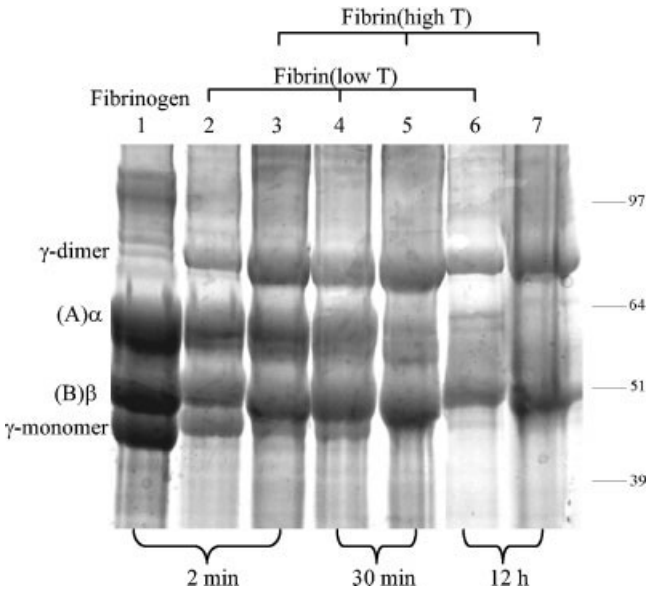

Figure 5. Reducing SDS-PAGE analysis of Tisseel® FS. Lane 1 represents the fibrinogen-containing solution, which contains Aα, Bβ, and γ-monomers with no appreciable γ-γ crosslinks. After the addition of 1.75 or 220 NIH U/mL of thrombin, polymerization reactions were stopped after 2 min (lanes 2 and 3), 30 min (lanes 4 and 5), and after 12 h (lanes 6 and 7). Over time, the intensity of the γ-monomer and of the α-monomer peaks decreased and the intensity of the γ-γ dimmer peaks increased. This indicates that both fibrin formations were highly crosslinked.

formulations may have resulted from different degrees of fibrin crosslinking mediated by factor XIIIa, which requires thrombin for its activation. Because factor XIIIa covalently links α-antiplasmin to fibrin and this renders the clot less resistant to plasmin degradation,[39] a highly crosslinked fibrin clot may impede cell invasion by reducing the ability of cells to degrade the fibrin. Moreover, it has been demonstrated that plasmin activity is an absolute requirement for fibroblasts to migrate into fibrin gels.[40] To investigate whether the differences observed between the two fibrin formulations could be explained by different degrees of fibrin crosslinking, reducing SDS-PAGE analysis was performed. After 12 h of polymerization, both fibrin formulations were highly crosslinked as evidenced by a significant reduction in α- and γ-monomers and by the formation of γ-γ crosslinks (Fig. 5). This suggests that the degree of fibrin crosslinking was not responsible for the observed *in vivo* differences. The variation in the fibrin structural properties between low T and high T groups likely influenced the *in vivo* response. Specifically, the larger pores in the fibrin(low T) samples likely permitted deeper penetration of cell processes versus the smaller pores in fibrin(high T). This, in turn, decreased the dependency on cell-mediated proteolysis of fibrin for penetration. Although not studied here, cell invasion may also be enhanced in matrices with larger pores due to facilitated diffusion of nutrients and of proteolysis factors such as tissue plasminogen activator, urokinase, and plasmin.[41] Shorter and thicker fibrin strands [as obtained with fibrin(low T)] may concentrate ligands and facilitate increased receptor-ligand avidity, which may also enhance cell migration.[42]

After 11 days, a similar amount of reparative bone was observed between the two fibrin-filled scaffold groups; however, much less bone occupied these defects compared with untreated defects and empty scaffolds ($p < 0.004$) (Figs. 4 and 6). It is possible that the supraphysiological concentration of fibrinogen (35–55 mg/mL) used for this study impeded cell invasion into the defects causing delayed bony wound healing given that the degree of neutrophil, macrophage, and fibroblast invasion into fibrin becomes significantly impeded above a fibrinogen concentration of 1–3 mg/mL.[43,44] Furthermore, it has been demonstrated *in vitro* for other cell types, such as neurons, that increasing the fibrinogen concentration above 5 mg/mL significantly reduces invasion.[45] Optimization of the fibrinogen concentration is likely necessary to achieve rapid cell infiltration and bone invasion throughout fibrin-filled scaffolds. In addition, the presence of aprotinin, which is a common additive in FS formulations,[29] blocks the conversion of plasminogen to plasmin and blocks the active site of plasmin; this may reduce cellular invasion and subsequently delay wound healing.[46]

It is possible that blocking the formation of a blood

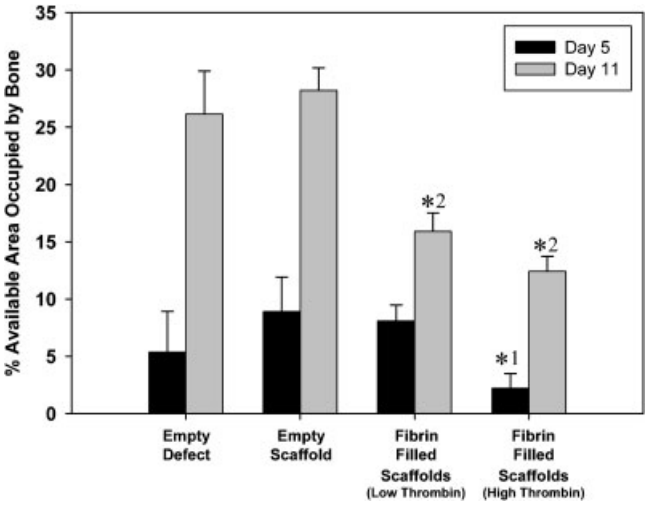

Figure 6. Histomorphometric analysis of reparative bone after 5 and 11 days *in vivo* ($n = 3$ or 4). After 5 days, no statistical differences were found between untreated defects, empty scaffolds, and fibrin-filled scaffolds containing fibrin(low T). However, significantly less bone was found in defects containing scaffolds filled with fibrin(high T) compared with empty scaffolds (*1: $p < 0.05$). After 11 days, both fibrin-filled scaffolds contained significantly less bone then the other two groups (*2: $p < 0.004$).

clot which contains many growth factors released from platelets, contributed to the lack of reparative bone found in scaffolds filled with FS at 11 days. However, Lutolf et al.[47] (2003) recently demonstrated that rat cranial critical-sized defects filled with a preformed poly(ethylene glycol)-based hydrogel matrix, which blocks blood clot formation, were completely infiltrated by cells and subsequently remodeled into bony tissue within 5 weeks. The mesh size in their synthetic gels was determined to be between 30–50 nm, which likely prevented blood cells from becoming entrapped in the defect site. Although not explicitly described, their experiment demonstrates the efficacy of a bone-healing strategy that involves filling a defect with a cell-invasive matrix, which blocks blood clot from becoming entrapped within the defect. In addition, they found that less bone invaded synthetic matrices of higher crosslink density. Similarly in our study, it is possible that the high crosslink density of both fibrin formulations (Fig. 5) significantly reduced bone invasion into the defects.

Commercially available FSs in their present state seem to be nonideal for bony wound-healing applications. Given that bone invasion at the early time point was affected by the fibrin structural properties, we believe the properties of FS can, and should, be tailored for their intended applications. Although no perfect matrix for filling scaffolds exists, one can elucidate the properties of an ideal pore-filling matrix by varying parameters such as crosslink density, fiber size, and pore size and studying the associated responses *in vivo*.

The authors thank Dr. Tania Benatar for technical advice, Professor John Weisel (University of Pennsylvania School of Medicine) for critically reviewing the manuscript, Professor David Courtman and Ms. Wanda Oprea for helpful discussions, Susan Carter for assistance during surgery, Dr. David Lickorish for providing Figure 1(C), and Franz Schuh for custom making our stainless steel cutting tools. This study was supported by an Ontario Research and Development Challenge Fund grant awarded to J. E. Davies and an Ontario Graduate Scholarship awarded to J. M. Karp.

References

1. Tajima M, Kuwahara S, Hirakawa S, Matsumoto K. Bone grafts using fibrin glue for posterolateral spinal fusion and total hip replacement with central migration. In: Redl H, Schlag G, editors. Fibrin sealing in surgical and nonsurgical fields. New York: Springer-Verlag; 1994. p 29–36.
2. Sielewicz M, Scholz J. Fibrin adhesive cancellous plasty in treating the dysplastic acetabulum in total joint replacement surgery: case report. In: Redl H, Schlag G, editors. Fibrin sealing in surgical and nonsurgical fields. New York: Springer-Verlag; 1994. p 37–43.
3. Marchetti N, Lisanti M, Scaglione M, Punzi G, Gabellieri P, Kufert J. Fibrin sealant in the treatment of infections in orthopedics. In: Redl H, Schlag G, editors. Fibrin sealing in surgical and nonsurgical fields. New York: Springer-Verlag; 1994. p 121–129.
4. Ferrari Parabita G, Derada Troletti GC, Cattaneo R, Ferrari Parabita S. The use of human fibrin glue in reconstructive maxillofacial surgery. In: Redl H, Schlag G, editors. Fibrin sealing in surgical and nonsurgical fields. New York: Springer-Verlag; 1994. p 139–146.
5. Schlag G, Redl H. Fibrin sealant in orthopedic surgery. Clin Orthop 1988;227:269–285.
6. Lasa CJ, Hollinger J, Drohan W, MacPhee MJ. Bone induction by demineralized bone powder and partially purified osteogenin using a fibrin-sealant carrier. In: Saltz R, Sierra DH, editors. Surgical adhesives and sealants: current technology and applications. Lancaster, PA: Technomic; 1996. p 135–143.
7. Urban K, Povysil C, Spelda S. [Effect of fibrin on osseointegration of bioactive glass-ceramic materials: experimental study]. Acta Chir Orthop Traumatol Cech 2001;68(3):168–175.
8. Oberg S, Kahnberg KE. Combined use of hydroxy-apatite and Tisseel in experimental bone defects in the rabbit. Swed Dent J 1993;17(4):147–153.
9. Cunin G, Boissonnet H, Petite H, Blanchat C, Guillemin G. Experimental vertebroplasty using osteoconductive granular material. Spine 2000;25(9):1070–1076.
10. Huang Q, Goh JC, Hutmacher DW, Lee EH. *In vivo* mesenchymal cell recruitment by a scaffold loaded with transforming growth factor beta1 and the potential for *in situ* chondrogenesis. Tissue Eng 2002;8(3):469–482.
11. Kawamura M, Urist MR. Human fibrin is a physiologic delivery system for bone morphogenetic protein. Clin Orthop 1988(235):302–310.
12. Yamada Y, Seong Boo J, Ozawa R, Nagasaka T, Okazaki Y, Hata K, Ueda M. Bone regeneration following injection of mesenchymal stem cells and fibrin glue with a biodegradable scaffold. J Craniomaxillofac Surg 2003;31(1):27–33.
13. van Susante JL, Buma P, Schuman L, Homminga GN, van den Berg WB, Veth RP. Resurfacing potential of heterologous chondrocytes suspended in fibrin glue in large full-thickness defects of femoral articular cartilage: an experimental study in the goat. Biomaterials 1999;20(13):1167–1175.
14. Bach AD, Bannasch H, Galla TJ, Bittner KM, Stark GB. Fibrin glue as matrix for cultured autologous urothelial cells in urethral reconstruction. Tissue Eng 2001;7(1):45–53.
15. Gurevich O, Vexler A, Marx G, Prigozhina T, Levdansky L, Slavin S, Shimeliovich I, Gorodetsky R. Fibrin microbeads for isolating and growing bone marrow-derived progenitor cells capable of forming bone tissue. Tissue Eng 2002;8(4):661–672.
16. Perka C, Schultz O, Spitzer RS, Lindenhayn K, Burmester GR, Sittinger M. Segmental bone repair by tissue-engineered periosteal cell transplants with bioresorbable fleece and fibrin scaffolds in rabbits. Biomaterials 2000;21(11):1145–1153.
17. Schantz JT, Teoh SH, Lim TC, Endres M, Lam CX, Hutmacher DW. Repair of calvarial defects with customized tissue-engineered bone grafts. I. Evaluation of osteogenesis in a three-dimensional culture system. Tissue Eng 2003;9(Suppl 1):S113–S126.
18. Schantz JT, Hutmacher DW, Lam CX, Brinkmann M, Wong KM, Lim TC, Chou N, Guldberg RE, Teoh SH. Repair of calvarial defects with customised tissue-engineered bone grafts. II. Evaluation of cellular efficiency and efficacy *in vivo*. Tissue Eng 2003;9(Suppl 1):S127–S139.
19. Senior RM, Skogen WF, Griffin GL, Wilner GD. Effects of fibrinogen derivatives upon the inflammatory response. Studies with human fibrinopeptide B. J Clin Invest 1986;77(3):1014–1019.
20. Leavell KJ, Peterson MW, Gross TJ. The role of fibrin degradation products in neutrophil recruitment to the lung. Am J Respir Cell Mol Biol 1996;14(1):53–60.

21. Thompson WD, Smith EB, Stirk CM, Marshall FI, Stout AJ, Kocchar A. Angiogenic activity of fibrin degradation products is located in fibrin fragment E. J Pathol 1992;168(1):47–53.
22. Albrektsson T, Bach A, Edshage S, Jonsson A. Fibrin adhesive system (FAS) influence on bone healing rate: a microradiographical evaluation using the bone growth chamber. Acta Orthop Scand 1982;53(5):757–763.
23. Schwarz N. The role of fibrin sealant in osteoinduction. Ann Chir Gynaecol Suppl 1993;207:63–68.
24. Bosch P, Lintner F, Arbes H, Brand G. Experimental investigations of the effect of the fibrin adhesive on the Kiel heterologous bone graft. Arch Orthop Trauma Surg 1980;96(3):177–185.
25. Carmagnola D, Berglundh T, Lindhe J. The effect of a fibrin glue on the integration of Bio-Oss with bone tissue. An experimental study in Labrador dogs. J Clin Periodontol 2002;29(5): 377–383.
26. Abiraman S, Varma HK, Umashankar PR, John A. Fibrin glue as an osteoinductive protein in a mouse model. Biomaterials 2002;23(14):3023–3031.
27. Kania RE, Meunier A, Hamadouche M, Sedel L, Petite H. Addition of fibrin sealant to ceramic promotes bone repair: long-term study in rabbit femoral defect model. J Biomed Mater Res 1998;43(1):38–45.
28. Brittberg M, Sjogren-Jansson E, Lindahl A, Peterson L. Influence of fibrin sealant (Tisseel) on osteochondral defect repair in the rabbit knee. Biomaterials 1997;18(3):235–242.
29. Jackson MR. Fibrin sealants in surgical practice: an overview. Am J Surg 2001;182(2 Suppl):1S–7S.
30. Ryan EA, Mockros LF, Weisel JW, Lorand L. Structural origins of fibrin clot rheology. Biophys J 1999;77(5):2813–2826.
31. Nehls V, Herrmann R. The configuration of fibrin clots determines capillary morphogenesis and endothelial cell migration. Microvasc Res 1996;51(3):347–364.
32. Amrani DL, Diorio JP, Delmotte Y. Wound healing. Role of commercial fibrin sealants. Ann NY Acad Sci 2001;936:566–579.
33. Carr ME. Fibrin formed in plasma is composed of fibers more massive than those formed from purified fibrinogen. Thromb Haemost 1988;59(3):535–539.
34. Karp JM, Rzeszutek K, Shoichet MS, Davies JE. Fabrication of precise cylindrical three-dimensional tissue engineering scaffolds for *in vitro* and *in vivo* bone engineering applications. J Craniofac Surg 2003;14(3):317–323.
35. Naito M, Nomura H, Iguchi A, Thompson WD, Smith EB. Effect of crosslinking by factor XIIIa on the migration of vascular smooth muscle cells into fibrin gels. Thromb Res 1998; 90(3):111–116.
36. Brown LF, Lanir N, McDonagh J, Tognazzi K, Dvorak AM, Dvorak HF. Fibroblast migration in fibrin gel matrices. Am J Pathol 1993;142(1):273–283.
37. Junquiera LC, Junqueira LC, Brentani RR. A simple and sensitive method for the quantitative estimation of collagen. Anal Biochem 1979;94(1):96–99.
38. Puchtler H, Waldrop FS, Valentine LS. Polarization microscopic studies of connective tissue stained with picro-sirius red FBA. Beitr Pathol 1973;150(2):174–187.
39. Sakata Y, Aoki N. Cross-linking of alpha 2-plasmin inhibitor to fibrin by fibrin-stabilizing factor. J Clin Invest 1980;65(2):290–297.
40. Knox P, Crooks S, Scaife MC, Patel S. Role of plasminogen, plasmin, and plasminogen activators in the migration of fibroblasts into plasma clots. J Cell Physiol 1987;132(3):501–508.
41. Diamond SL, Anand S. Inner clot diffusion and permeation during fibrinolysis. Biophys J 1993;65(6):2622–2643.
42. van Kooyk Y, Figdor CG. Avidity regulation of integrins: the driving force in leukocyte adhesion. Curr Opin Cell Biol 2000; 12(5):542–547.
43. Ciano PS, Colvin RB, Dvorak AM, McDonagh J, Dvorak HF. Macrophage migration in fibrin gel matrices. Lab Invest 1986; 54(1):62–70.
44. Hanson AJ, Quinn MT. Effect of fibrin sealant composition on human neutrophil chemotaxis. J Biomed Mater Res 2002;61(3): 474–481.
45. Herbert CB, Nagaswami C, Bittner GD, Hubbell JA, Weisel JW. Effects of fibrin micromorphology on neurite growth from dorsal root ganglia cultured in three-dimensional fibrin gels. J Biomed Mater Res 1998;40(4):551–559.
46. Krishnan LK, Vijayan Lal A, Uma Shankar PR, Mohanty M. Fibrinolysis inhibitors adversely affect remodeling of tissues sealed with fibrin glue. Biomaterials 2003;24(2):321–327.
47. Lutolf MP, Weber FE, Schmoekel HG, Schense JC, Kohler T, Muller R, Hubbell JA. Repair of bone defects using synthetic mimetics of collagenous extracellular matrices. Nat Biotechnol 2003;21(5):513–518.